

Amelogenin binds to both heparan sulfate and bone morphogenetic protein 2 and pharmacologically suppresses the effect of noggin

Kan Saito, Ikuri Konishi, Miyuki Nishiguchi, Tomonori Hoshino* and Taku Fujiwara

Division of Pediatric Dentistry, Nagasaki University Graduate School of Biomedical Sciences, 1-7-1 Sakamoto, Nagasaki 852-8588, Japan

Tel.: +81 95 819 7674

Fax: +81 95 819 7676

*Corresponding author: thoshino@nagasaki-u.ac.jp

Abstract

Enamel matrix derivative (EMD) is widely considered useful to promote tissue regeneration during periodontal treatment. It has been reported that the main constituent of EMD is amelogenin and that the BMP-like and TGF- β -like activity of EMD promotes osteogenesis. However, it remains unclear whether those activities are dependent on amelogenin or another growth factor contained in EMD. We performed two-dimensional SDS-PAGE analysis of EMD, as well as Western blot analyses using anti-amelogenin, anti-BMP2/4, and anti-TGF- β 1 antibodies, and amino acid sequencing. Our results revealed that a large number of splicing forms of amelogenin, BMP2/4, and other unknown molecules were involved in EMD, though TGF- β 1 was not. In addition, we have evaluated intracellular signaling of ERK1/2 and Smad1/5/8, binding potential and alkaline phosphatase activity and have explored the potential regulatory relationship between amelogenin and BMP. Amelogenin bound to BMP2 as well as heparin/heparan sulfate. Thus, it was suggested that BMP2/4 carried over in EMD during processing promote binding activity and phosphorylate Smad1/5/8 in osteoblasts. On the other hand, amelogenin did not phosphorylate Smad1/5/8, but rather

ERK1/2. Further, high density amelogenin reduced the inhibition of alkaline phosphatase activity by noggin, though amelogenin did not have antagonistic properties against BMP. Together with the above findings, our findings suggest that the BMP2/4 contaminated during the purification process of EMD because of the avidity of amelogenin plays an important role in signaling pathway of calcification.

Key words: amelogenin, BMP, noggin, osteoblast, heparan sulfate

Introduction

Enamel matrix derivative (EMD) is derived from developing porcine teeth. A recent clinical review reported that EMD promotes both cementogenesis [1] and osteogenesis [2], while it has also been shown that EMD has bone morphogenetic protein (BMP) and transforming growth factor- β (TGF- β) activities [3, 4], while *in vitro* experiments demonstrated that it stimulates osteoblast proliferation and differentiation [5, 6]. EMD consists of amelogenin at nearly 90%, along with other enamel matrix proteins, such as enamelin, tuftelin, amelin, and ameloblastin [7, 8]. Amelogenin is expressed in a tissue-specific manner by ameloblast, of which the origin is ectoderm. Immature enamel contains a complex mixture of amelogenin polypeptides, primarily due to the combined effects of alternative splicing [9, 10]. Numerous mutations have been found in the genes encoding amelogenin in patients with amelogenesis imperfecta, the most common genetic disorder affecting enamel [11, 12]. Thus, it is thought that amelogenin plays a crucial role in enamel formation. On the other hand, though there is no known clinical report showing that amelogenin causes bone diseases, *in vitro* experiment results have provided some indications of its function in bone formation. For example,

leucine-rich amelogenin peptide (LRAP) is expressed in cementoblasts/periodontal ligament cells and regulates osteoclastogenesis [13], and was shown to down-regulate osteocalcin, a marker of bone turnover [14, 15]. In another study, amelogenin decreased the levels of RANKL, M-CSF, and fibronectin in osteoblasts [16]. However, it remains unknown whether the activity of amelogenin is equal to that of EMD in bone formation. In the present study, we investigated EMD using two-dimensional SDS-PAGE assays and Western blot analyses to determine the differences between EMD and amelogenin. Our findings revealed that BMP2/4 contaminated EMD during processing. We also examined ERK1/2 and Smad1/5/8 intracellular signaling, the binding properties of amelogenin for BMP2, heparin, and heparan sulfate, and the alteration of alkaline phosphatase activity by amelogenin during calcification, to determine the relationship between amelogenin and BMP.

Materials and methods

Two-dimensional SDS-PAGE (2-D PAGE) and Western blot analyses

The commercial enamel matrix derivative Emdogain[®], extracted from developing porcine teeth, was purchased from Seikagaku-kougyou Corporation (Tokyo, Japan) and used in the experiments. Approximately 5 µg of protein was added to 155 µL of sample rehydration buffer and absorbed overnight onto 7-cm nonlinear immobilized pH gradient (IPG, pH 3–10) ZOOM strips (Invitrogen Corp., Carlsbad, CA). Isoelectric focusing was carried out using a ZOOM[®] IPG Runner system (Invitrogen) and a MAJOR SCIENCE MP–3500/250P power supply (Invitrogen) with the following voltage step protocol: 200 V for 15 minutes, 450 V for 15 minutes, 750 V for 15 minutes, and 2000 V for 60 minutes. For the second dimension, focused IPG strips were equilibrated in NuPAGE[®] LDS sample buffer (Invitrogen) in the presence of NuPAGE[®] Sample Reducing Agent (Invitrogen) for 15 minutes, and then further incubated in LDS sample buffer in the presence of 125 mM iodoacetamide for 15 minutes. Next, the strips were placed on NuPAGE[®] 4–12% Bis–Tris gels (Invitrogen) and embedded in 0.5%

agarose (wt/vol).

Coomassie brilliant blue (CBB) staining of the gels was performed using SimplyBlue SafeStain™ (Invitrogen). For immunoblotting, proteins were separated using 2-D PAGE and transferred to 0.2- μ m polyvinylidene fluoride (PVDF) membranes (Invitrogen) for 30 minutes at a constant 200 V. After blocking with 5% nonfat dry milk and 0.2% Tween 20 in Tris borate saline (TBS) at 4°C overnight, the membranes were incubated with rabbit anti-amelogenin (anti-AMEL; HOKUDO CO., LTD, Sapporo, Japan), goat anti-BMP2/4 (R&D systems, Minneapolis, MN), or mouse anti-human TGF- β 1 (R&D systems) antibodies in TBS containing 1% bovine serum albumin for 1 hour at room temperature. The antibodies were used at a dilution of 1:1000. The membranes were washed 5 times with TBS containing 0.2% Tween and then incubated with secondary antibodies at a dilution of 1:3000 in TBS with 1% bovine serum albumin for 1 hour at room temperature. The membranes were then washed 5 times with TBS and signals were detected using an ECL kit (Amersham Pharmacia Biosciences, Uppsala, Sweden).

Analyses of 2-D gel and Western blotting results

CBB-stained gels were scanned at 500 dpi and the images analyzed using Progenesis PG200 Software (Nonlinear Dynamics, Newcastle upon Tyne, UK) to determine the number, molecular weight, isoelectric point, and relative volume ratio of the molecules in EMD. After normalization based on total spot density was performed, the relative volume of individual spots was calculated and quantified by the intensity of staining. After Western blotting images were also scanned at 500 dpi, the signals on the ECL film were merged and calibrated to the spots on gels stained with SimplyBlue SafeStain™.

Preparation of recombinant mouse amelogenin

To construct a plasmid expressing amelogenin, cDNA was amplified by PCR. The amplified DNA fragment was cloned into the *Bam*HI-*Xho*I region of pET22b (+) (Novagen, Darmstadt, Germany), which allowed the expressed amelogenin protein to fuse to the poly-histidine tag at the C-terminus. Recombinant amelogenin (rAMEL) was expressed as an insoluble inclusion body in *E. coli* BL21 harboring the plasmid by

treatment with isopropylthio- β -D-thiogalactoside, and was solubilized in 20 mM sodium phosphate buffer (NaPB) containing 0.5 M NaCl and 6 M guanidine hydrochloride. The solubilized rAMEL was purified by Ni²⁺-chelate affinity chromatography using a ProBondTM resin column (Invitrogen) according to the manufacturer's instructions. Briefly, crude rAMEL was applied to the column and eluted with 20 mM NaPB containing 8M urea and 0.1% Triton-X100. The purified fractions were dialyzed against 20 mM NaPB (pH 4.0) containing 0.1% Triton-X100 to remove the urea. Removal of lipopolysaccharide (LPS) was accomplished by Triton X-114 (SIGMA, St. Louis, MO) [17]. The rAMEL used in this study contained less than 1 pg of LPS per 1 μ g of protein.

Cell culture and signaling assay

The mouse osteoblast cell line MC3T3-E1 was obtained from RIKEN Cell Bank (Tsukuba, Japan). Cells were maintained in α -MEM (SIGMA) containing 10% fetal bovine serum (FBS; Invitrogen) and 100 units/mL of penicillin-G at 37°C in a humidified atmosphere of 5% CO₂ in air. Cultured MC3T3-E1 cells were treated with 5

$\mu\text{g/mL}$ of EMD, $5 \mu\text{g/mL}$ of rAMEL and 100 ng/mL of recombinant BMP2 (Genzyme/Techne, Cambridge, MA) for 0 to 60 minutes. Treated cells were washed with phosphate buffered saline (PBS) containing $1 \text{ mM Na}_3\text{VO}_4$, and then solubilized in $200 \mu\text{L}$ of lysis buffer [10 mM Tris-HCl (pH 7.4), 150 mM NaCl , 10 mM MgCl_2 , 0.5% Nonidet P-40, $1 \text{ mM phenylmethylsulfonyl fluoride}$, $20 \text{ units/mL aprotinin}$). The lysed cell solution was centrifuged at $12,000 \times g$ for 10 minutes and the supernatants recovered were used as samples to assay cell signaling. The protein concentration of each sample was measured using Lowry's method. After the samples were separated on NuPAGE[®] 4–12% Bis-Tris gels (Invitrogen), the gels were transferred onto PVDF membranes. To assay cell signaling during phosphorylation, the membranes were analyzed by Western blotting using anti-phospho ERK1/2 (p-ERK1/2), anti-ERK1/2, anti-phospho Smad1/5/8 (p-Smad1/5/8), and Smad5 antibodies (Cell Signaling Technology, Beverly, MA)

Amino acid sequence of characteristic spots on 2-D gels

Separated EMD samples on 2-D gels were blotted onto PVDF membranes. Then,

characteristic spots on the 2-D gels were excised from the blotted membranes and subjected to sequencing using a Procise 492cLC (Applied Biosystems, Foster City, CA.). Homology searches of the resultant sequences were performed using protein-protein BLAST (blastp) located on the web site of the National Center for Biotechnology Information (<http://www.ncbi.nlm.nih.gov/BLAST/>).

Assay of binding between amelogenin and BMP2

0 to 1.0 μg of rAMEL was dissolved in PBS and added to 100 ng of BMP2 in a final volume of 250 μL and incubated at 4°C for 8 hours. Following incubation, 0.25 μL of Ni^{2+} -chelate ProbondTM resin (Invitrogen) was added to the reaction mixture and incubated at 4°C for 8 hours. Resin beads were recovered by centrifugation and washed 5 times with 1000 μL of PBS. The opposite way for the above reaction was also analysed. 100 ng of rAMEL was dissolved in PBS and added to 0 to 500 ng of BMP2 in a final volume of 250 μL and incubated at 4°C for 8 hours. The resulting complexes were immunoprecipitated using anti-BMP 2/4 antibody coupled with protein G plus protein A agarose (Calbiochem, Darmstadt, Germany) at 4°C for 1 hour. These

precipitates were suspended in NuPAGE[®] LDS sample buffer and applied to NuPAGE[®] 4–12% Bis–Tris gels. The gels were electrophoresed gel and blotted onto PVDF membranes, then subjected to immunostaining respectively using the anti–BMP2/4 and anti-AMEL antibody, as described above.

Analyses of binding affinity of rAMEL for heparin and heparan sulfate

5 µg of rAMEL was mixed with 0 to 200 µg of heparin acrylic beads or 0 to 100 µg of heparan sulfate in 500 µL of binding buffer (25 mM Tris–HCl (pH 7.5), 0.1 M NaCl, 0.1% CHAPS) and incubated at 4°C for 8 hours. Acrylic beads (200 µg) (Sephacryl[®] 100–HR; SIGMA) were used as a negative control to prevent the binding of rAMEL to the beads themselves. Following incubation, the heparin beads were recovered by centrifugation and washed 5 times with 200 µL of binding buffer. The binding affinity of rAMEL for heparin was detected using Western blotting analyses of reaction intensity against the anti–AMEL antibody. For the analysis of the intensity of binding of rAMEL to heparin, 0.2 to 1.0 M NaCl was added to the above binding buffer, and the intensity was evaluated by the concentration of NaCl when binding. In the

binding affinity of rAMEL for heparan sulfate, the free rAMEL, which did not bound to heparan sulfate in the rAMEL–heparan sulfate complex mixture, was recovered by heparin beads and analyzed by using the same protocol.

Assay of alkaline phosphatase activity

MC3T3–E1 cells were cultured in the presence of 50 ng/mL of BMP2 and various concentrations of rAMEL with or without 400 ng/mL of noggin (R&D Systems) for 14 days. Assays of alkaline phosphatase (ALP) activity were performed with a TRACP & ALP Assay Kit[®] (Takara, Tokyo, Japan), according to the manufacturer's instructions.

Inhibition of binding between BMP2 and noggin by rAMEL

rAMEL (0–5 µg) was mixed with 1 µg of BMP2 and 100 ng of noggin in 500 µL of binding buffer and incubated at 4°C for 8 h. The resulting complexes were immunoprecipitated using anti–BMP 2/4 antibody coupled with protein G plus protein

A agarose (Calbiochem, Darmstadt, Germany) at 4°C for 1 h. The precipitates were electrophoresed, transferred to PVDF membranes, and immunoassayed using anti-noggin antibody (R&D Systems).

Statistical analysis

Triplicate samples were analyzed in each experiment, with each replicated to ensure consistency of the responses to amelogenin. Significant differences were determined using Student's *t* test.

Results

EMD contains amelogenin and BMP2/4, but not TGF- β

A previous report found that EMD prepared from developing porcine teeth possesses BMP-like and TGF- β -like activities [3, 4], though the molecular mechanism is uncertain. To obtain detailed findings regarding the molecules contained in EMD, we performed 2-D PAGE analysis of EMD protein using a Zoom IPG Runner System (see materials and methods section).

Primary spots were detected in the area with a molecular weight (MW) ranging from 3 to 25 kDa and an isoelectric point (pI) ranging from 6.2 to 10 (Fig. 1A). At around 22 kDa and pI 7.0, a large number of high-density spots were found, which were identified as full-length amelogenin by Western blot analysis probed with the rabbit polyclonal anti-AMEL antibody (Fig. 1B). In our Western blotting analysis using the goat polyclonal anti-BMP2/4 antibody, clearly positive spots were seen in a range of 80 kDa/pI 7.6–8.2 and 110 kDa/pI 7.2–7.5 (Fig. 1C). Western blot analysis using the anti-TGF- β 1 was also carried out, however, no detectable protein was observed that

interacted with that antibody (data not shown).

Amelogenin enhances phosphorylation of ERK, but not Smad, in MC3T3–E1 osteoblasts

Since our results demonstrated that EMD contains BMP proteins, we compared the ability to activate cell signaling in MC3T3–E1 osteoblasts among EMD, purified rAMEL, and BMP2. The obtained rAMEL at 5 µg/mL induced phosphorylation of ERK–1/2 (Fig. 2A), which demonstrated that the rAMEL was physiologically intact. Consistent with a previous study of fibroblasts [18], stimulation with 5 µg/mL of EMD also induced ERK–1/2 phosphorylation. These results suggest that amelogenin, which comprises more than 90% of EMD, is the molecule involved in activation of the ERK pathway when osteoblasts are stimulated with EMD.

On the other hand, the phosphorylation of Smad was observed when BMP2 or EMD and not rAMEL was added (Fig. 2B). Therefore, we speculated that the BMP–like activity of EMD is not dependent on amelogenin, but rather the BMP protein contained in EMD.

Imaging analysis of 2-D PAGE spots and amino acid sequence of two unknown fractions

Figure 1D shows results of imaging analysis of 2-D PAGE and Western blotting assays. Those results led us to determine the molecules that equalled 19.5% of the total that did not interact with the anti-AMEL and anti-BMP2/4 antibodies.

We attempted to identify the unknown fractions detected as two different spots with comparatively intense signals, indicated by arrowheads in Figure 1D. The N-terminal 20 amino acids sequence of those were revealed to be MPLPPHPGHPGYINFSYEVL and MPLPPHPGHPGYINFFYEVL, and showed a similarity to amelogenin in a blastp homology search.

Amelogenin binds to BMP

Figure 1D revealed that the yellow spots occupied 6.8% of EMD reacted to both anti-AMEL and anti-BMP2/4 antibodies. Thus, we speculated that amelogenin possess

the binding activity to BMP. To confirm this finding, we examined the interaction of amelogenin and BMP2 *in vitro* using a protein binding assay (Fig. 3). Poly-histidine tagged rAMEL was incubated with Ni-beads and BMP2 prepared from CHO cells. The mixture of rAMEL and Ni-beads was negative in subsequent immunoblot analysis using anti-BMP2/4 antibody. With regard to the mixture of rAMEL, BMP2, and Ni-beads, a positive band against the anti-BMP2/4 antibody was observed when more than 0.5 µg of rAMEL was added, and the intensity of the band increased in a concentration-dependent manner (Fig. 3A). Then, the binding activity between rAMEL and BMP2 was also observed in the opposite way for the above (Fig. 3B). As the result, it was developed that the binding intensity increased just like the above mentioned. From these results, the interaction between amelogenin and BMP2 was confirmed.

Amelogenin binds to heparin/heparan sulfate

It is well known that both growth factors such as BMP2/4 and extracellular matrix to interact with heparin/heparan sulfate [19, 20]. Since the molecular weight of the amelogenin-BMP merged spots was greater than the sum of each individually and, we

speculated that heparan sulfate was involved in amelogenin–BMP molecular interactions.

First, to confirm the binding of amelogenin and heparin, we precipitated rAMEL with heparin beads. The precipitation of rAMEL by the heparin beads occurred in a concentration–dependent manner; however, this was not observed in the case of rAMEL precipitation by the acrylic beads (Fig. 4A). In the examination of the avidity between rAMEL and heparin, the addition of more than 0.9 M NaCl decreased binding activity (Fig. 4B). These results suggest that amelogenin binds to heparin *in vivo*. The complex of rAMEL and heparin was competitively decreased by the addition of heparan sulfate (Fig. 4C). Thus, it was demonstrated that rAMEL binds to not only the heparin but also the heparan sulfate.

Amelogenin promotes BMP function following noggin suppression

When it was based on the hypothesis that amelogenin possess the binding activity to BMP, it was interesting whether amelogenin act as agonist or antagonist on the ALP activity associated with BMP. As shown in Figure 5A, the addition of rAMEL did not

inhibit up-regulation of ALP activity in MC3T3-E1 cell by BMP2. On the other hand, it was reported that the addition of noggin inhibited acceleration of ALP activity by BMP2 as reported formerly [21]. When examining the effect of amelogenin on this inhibition by noggin, a low concentration of rAMEL did not depress the effect of noggin. However, the ALP activity associated with BMP was recovered by adding more than 10 $\mu\text{g}/\text{mL}$ of rAMEL (Fig. 5B).

Amelogenin inhibits binding of noggin to BMP2

Based on the observation that rAMEL repressed the inhibition of BMP-associated ALP activity by noggin (Figure 5B), it was speculated that amelogenin inhibited the binding between BMP2 and noggin. Thus, we investigated whether rAMEL inhibited the binding between BMP2 and noggin by immunoprecipitation. It was found that rAMEL inhibited the binding between BMP2 and noggin when it was added at a concentration that was 10-fold greater than that of noggin (Fig. 6). This ratio between the concentrations of amelogenin and noggin supported the result shown in Figure 5B.

Discussion

All splicing forms, such as tyrosine-rich amelogenin (TRAP) and leucine-rich amelogenin (LRAP), have different functions and are expressed in various tissues [22, 23]. In the present study, CBB staining indicated that EMD could be separated into 46 proteins, and spots that reacted with the anti-AMEL antibody were observed in a MW range from 8 to 24 kDa and a pI range from 7.2 to 9.3 (Fig. 1B). These results confirmed those of the previous report about the component of EMD using anti-AMEL antibody, which revealed that EMD was composed mainly of amelogenin and that EMD contains many splicing form of amelogenin ranging 10 to 40 kDa with the majority components at 20 kDa [24]. In this report, the western blotting analyses of EMD using anti-amelin, anti-enamelin, and anti-albumin antibodies were also carried out and revealed that no cross-reactivity was seen. However, although EMD has BMP and TGF- β activity [3, 4], there is no report concerning the western blotting analyses of EMD using anti-BMP and anti-TGF- β antibodies. Thus, we performed the immunoblot analyses using these antibodies.

Immunoblot analysis showed that EMD derived from porcine samples did not react

with the anti-human TGF- β 1 antibody (data not shown). According to the manufacturer's instructions, the anti-human TGF- β 1 antibody used in this study reacts with TGF- β 1 derived from humans, rats, and mice. The amino acid sequence homology between porcine TGF- β 1 and that of those is 94%, 89%, and 89%, respectively. In a phylogenetic tree from those animal species based on the neighbor-joining method, porcine TGF- β 1 is located between that of humans and rodents, and belongs to the same cluster as human TGF- β 1 (data not shown). Therefore, the possibility that porcine TGF- β 1 does not react with the tested anti-TGF- β 1 antibody is very low. Thus, it is suggested that TGF- β 1 is not involved with EMD and that amelogenin or other molecules in EMD may possess TGF- β -like activities.

Positive fractions were detected in our Western blot analysis of EMD with the anti-BMP2/4 antibody (Fig. 1C). Expression of BMP was reported to be shifted between epithelium and mesenchyme during the tooth initiation stage, and remarkable associations with epithelial-mesenchymal interactions were shown [25]. In addition, we confirmed that amelogenin binds to BMP2 (Fig. 3). Thus, it is suggested that the BMP-like molecule is retained during the purification process of EMD due to this binding ability of amelogenin.

BMP2/4 induce differentiation of osteoblasts [26] and belong to the TGF- β family

of proteins that act as potent osteogenic morphogens capable of inducing calcification in animal models [27]. Thus, we examined the effects of EMD and single rAMEL on the Smad phosphorylation induced by BMP2, which was an important signaling pathway in calcification. We found that the phosphorylation of Smad 1/5/8 was not induced by amelogenin alone, but rather by whole EMD (Fig. 2C), indicating that amelogenin does not inhibit BMP signaling. Thus, it was suggested that the BMP-like molecule in EMD, which might be the precursor of BMP at its molecular weight, induced the phosphorylation of Smad. It was reported that bone inducing activity was displayed by proBMP2 [28]. Therefore, it is suggested that EMD extracted from porcine tooth germ tissue has a pharmacological effect on bone formation and periodontal reproduction, based on its contamination with trace amounts of active BMP.

Heparin/heparan sulfate binds to growth factors, including BMP, the fibroblast growth factor (FGF) family, heparin-binding epidermal growth factor, and vascular endothelial growth factor [19, 29–31], as well as to extracellular matrix molecules such as fibronectin, vitronectin, and laminin [20]. Proteoglycans have been identified within bone extracellular matrices and are known to play a role in mineralization and bone formation. BMP2-induced osteoblasts induce the synthesis of secreted chondroitin/dermatan sulfate proteoglycans and heparan sulfate proteoglycans

associated with the cell and its environment [32]. Heparin enhances BMP2-induced gene expression and Smad1/5/8 phosphorylation. Noggin failed to inhibit BMP2 activity in the presence of heparin [33]. Sulfated polysaccharides enhance the biological activity of BMP dimers by continuous delivery of the ligands to their signaling receptors expressed on cell membranes [34]. Based on those results, we speculated that amelogenin, an extracellular matrix molecule, would bind to heparin/heparan sulfate, which was confirmed in the present experiments (Fig. 4A). It has also been reported that FGF binding to heparin was abrogated by 0.5 to 0.9 M NaCl [35, 36] and amelogenin binding to heparin was dissociated in 0.9 M NaCl in the present study (Fig. 4B). Thus, it was revealed that the avidity between amelogenin and heparin is the same as that between FGF and heparin. Further, we found that amelogenin binds to not only heparin, but also heparan sulfate (Fig. 4C). These results suggest that amelogenin contributes to bone formation via binding to heparan sulfate.

It was previously reported that BMP2 can bind to other molecules such as noggin, chordin, follistatin, and biglycan [37–40]. It was also reported that noggin has an ability to bind to heparan sulfate and functions as an antagonist of BMP [21, 41]. On the other hand, the present results indicate that amelogenin possesses the ability to bind to both BMP2 and heparan sulfate. However, the influence of amelogenin on calcification by

BMP has not been reported. Thus, amelogenin was added to the present experimental system, in which the up-regulation of alkaline phosphatase activity by BMP was inhibited by noggin, and high density amelogenin rescued the inhibited calcification (Fig. 5). The result in Figure 6 indicates that amelogenin inhibited binding of noggin to BMP2 and that BMP2 become functionally free. These results suggest that a high concentration of amelogenin may be effective for use as a therapeutic agent for promoting bone formation, though such concentrations do not exist *in vivo*.

In conclusion, our findings indicate that the BMP-like activity of EMD is derived from trace amounts of BMP2/4 carried over during the production process, and caused by the ability of amelogenin to bind to BMP. Moreover, since amelogenin suppressed the inhibition of the BMP-induced ALP activity by noggin, amelogenin may be pharmacologically effective for promoting bone formation.

Acknowledgement

This work was supported by grants-in-aid from the Japan Society for the Promotion of Science (No. 19791588, 18592243).

References

- [1] Hammarstrom L. Enamel matrix, cementum development and regeneration. *J Clin Periodontol* 1997;24: 658–68.
- [2] Venezia E, Goldstein M, Boyan BD, Schwartz Z. The use of enamel matrix derivative in the treatment of periodontal defects: a literature review and meta-analysis. *Crit Rev Oral Biol Med* 2004;15: 382–402.
- [3] Kawase T, Okuda K, Momose M, Kato Y, Yoshie H, Burns DM. Enamel matrix derivative (EMDOGAIN) rapidly stimulates phosphorylation of the MAP kinase family and nuclear accumulation of smad2 in both oral epithelial and fibroblastic human cells. *J Periodontal Res* 2001;36: 367–76.
- [4] Suzuki S, Nagano T, Yamakoshi Y, Gomi K, Arai T, Fukae M, Katagiri T, Oida S. Enamel matrix derivative gel stimulates signal transduction of BMP and TGF- β . *J Dent Res* 2005;84: 510–4.
- [5] He J, Jiang J, Safavi KE, Spangberg LS, Zhu Q. Emdogain promotes osteoblast proliferation and differentiation and stimulates osteoprotegerin expression. *Oral Surg Oral Med Oral Pathol Oral Radiol Endod* 2004;97: 239–45.
- [6] Keila S, Nemcovsky CE, Moses O, Artzi Z, Weinreb M. In vitro effects of

enamel matrix proteins on rat bone marrow cells and gingival fibroblasts. *J Dent Res* 2004;83: 134–8.

[7] Termine JD, Belcourt AB, Christner PJ, Conn KM, Nylen MU. Properties of dissociatively extracted fetal tooth matrix proteins. I. Principal molecular species in developing bovine enamel. *J Biol Chem* 1980;255: 9760–8.

[8] Robinson C, Brookes SJ, Shore RC, Kirkham J. The developing enamel matrix: nature and function. *Eur J Oral Sci* 1998;106 Suppl 1: 282–91.

[9] Lau EC, Simmer JP, Bringas P, Jr., Hsu DD, Hu CC, Zeichner–David M, Thiemann F, Snead ML, Slavkin HC, Fincham AG. Alternative splicing of the mouse amelogenin primary RNA transcript contributes to amelogenin heterogeneity. *Biochem Biophys Res Commun* 1992;188: 1253–60.

[10] Li R, Li W, DenBesten PK. Alternative splicing of amelogenin mRNA from rat incisor ameloblasts. *J Dent Res* 1995;74: 1880–5.

[11] Wright JT, Hall KI, Yamauche M. The enamel proteins in human amelogenesis imperfecta. *Arch Oral Biol* 1997;42: 149–59.

[12] Collier PM, Sauk JJ, Rosenbloom SJ, Yuan ZA, Gibson CW. An amelogenin gene defect associated with human X–linked amelogenesis imperfecta. *Arch Oral Biol* 1997;42: 235–42.

- [13] Hatakeyama J, Philp D, Hatakeyama Y, Haruyama N, Shum L, Aragon MA, Yuan Z, Gibson CW, Sreenath T, Kleinman HK, Kulkarni AB. Amelogenin-mediated Regulation of Osteoclastogenesis, and Periodontal Cell Proliferation and Migration. *J Dent Res* 2006;85: 144–9.
- [14] Boabaid F, Gibson CW, Kuehl MA, Berry JE, Snead ML, Nociti FH, Jr., Katchburian E, Somerman MJ. Leucine-rich amelogenin peptide: a candidate signaling molecule during cementogenesis. *J Periodontol* 2004;75: 1126–36.
- [15] Swanson EC, Fong HK, Foster BL, Paine ML, Gibson CW, Snead ML, Somerman MJ. Amelogenins regulate expression of genes associated with cementoblasts in vitro. *Eur J Oral Sci* 2006;114 Suppl 1: 239–43.
- [16] Nishiguchi M, Yuasa K, Saito K, Fukumoto E, Yamada A, Hasegawa T, Yoshizaki K, Kamasaki Y, Nonaka K, Fujiwara T, Fukumoto S. Amelogenin is a negative regulator of osteoclastogenesis via downregulation of RANKL, M-CSF and fibronectin expression in osteoblasts. *Arch Oral Biol* 2007;52: 237–43.
- [17] Liu S, Tobias R, McClure S, Styba G, Shi Q, Jackowski G. Removal of endotoxin from recombinant protein preparations. *Clin Biochem* 1997;30: 455–63.
- [18] Zeldich E, Koren R, Nemcovsky C, Weinreb M. Enamel matrix derivative stimulates human gingival fibroblast proliferation via ERK. *J Dent Res* 2007;86: 41–6.

- [19] Ruppert R, Hoffmann E, Sebald W. Human bone morphogenetic protein 2 contains a heparin-binding site which modifies its biological activity. *Eur J Biochem* 1996;237: 295–302.
- [20] Cool SM, Nurcombe V. The osteoblast–heparan sulfate axis: control of the bone cell lineage. *Int J Biochem Cell Biol* 2005;37: 1739–45.
- [21] Zimmerman LB, De Jesus–Escobar JM, Harland RM. The Spemann organizer signal noggin binds and inactivates bone morphogenetic protein 4. *Cell* 1996;86: 599–606.
- [22] Hatakeyama J, Sreenath T, Hatakeyama Y, Thyagarajan T, Shum L, Gibson CW, Wright JT, Kulkarni AB. The receptor activator of nuclear factor–kappa B ligand–mediated osteoclastogenic pathway is elevated in amelogenin–null mice. *J Biol Chem* 2003;278: 35743–8.
- [23] Paine ML, Zhu DH, Luo W, Snead ML. Overexpression of TRAP in the enamel matrix does not alter the enamel structural hierarchy. *Cells Tissues Organs* 2004;176: 7–16.
- [24] Maycock J, Wood SR, Brookes SJ, Shore RC, Robinson C, Kirkham J. Characterization of a porcine amelogenin preparation, EMDOGAIN, a biological treatment for periodontal disease. *Connect Tissue Res* 2002;43: 472–6.

- [25] Aberg T, Wozney J, Thesleff I. Expression patterns of bone morphogenetic proteins (Bmps) in the developing mouse tooth suggest roles in morphogenesis and cell differentiation. *Dev Dyn* 1997;210: 383–96.
- [26] Ghosh–Choudhury N, Harris MA, Feng JQ, Mundy GR, Harris SE. Expression of the BMP 2 gene during bone cell differentiation. *Crit Rev Eukaryot Gene Expr* 1994;4: 345–55.
- [27] Wozney JM, Rosen V. Bone morphogenetic protein and bone morphogenetic protein gene family in bone formation and repair. *Clin Orthop Relat Res* 1998: 26–37.
- [28] Hillger F, Herr G, Rudolph R, Schwarz E. Biophysical comparison of BMP–2, ProBMP–2, and the free pro–peptide reveals stabilization of the pro–peptide by the mature growth factor. *J Biol Chem* 2005;280: 14974–80.
- [29] Higashiyama S, Lau K, Besner GE, Abraham JA, Klagsbrun M. Structure of heparin–binding EGF–like growth factor. Multiple forms, primary structure, and glycosylation of the mature protein. *J Biol Chem* 1992;267: 6205–12.
- [30] Folkman J, Shing Y. Control of angiogenesis by heparin and other sulfated polysaccharides. *Adv Exp Med Biol* 1992;313: 355–64.
- [31] Jackson RA, Nurcombe V, Cool SM. Coordinated fibroblast growth factor and heparan sulfate regulation of osteogenesis. *Gene* 2006;379: 79–91.

- [32] Gutierrez J, Osses N, Brandan E. Changes in secreted and cell associated proteoglycan synthesis during conversion of myoblasts to osteoblasts in response to bone morphogenetic protein-2: role of decorin in cell response to BMP-2. *J Cell Physiol* 2006;206: 58–67.
- [33] Zhao B, Katagiri T, Toyoda H, Takada T, Yanai T, Fukuda T, Chung UI, Koike T, Takaoka K, Kamijo R. Heparin potentiates the in vivo ectopic bone formation induced by bone morphogenetic protein-2. *J Biol Chem* 2006;281: 23246–53.
- [34] Takada T, Katagiri T, Ifuku M, Morimura N, Kobayashi M, Hasegawa K, Ogamo A, Kamijo R. Sulfated polysaccharides enhance the biological activities of bone morphogenetic proteins. *J Biol Chem* 2003;278: 43229–35.
- [35] Gambarini AG, Miranda MT, Viviani W, Oyama Junior S, Kiyota S, Toma IN. Structure and function of fibroblast growth factor. *Braz J Med Biol Res* 1996;29: 835–9.
- [36] Emoto N, Shimizu K, Onose H, Ishii S, Sugihara H, Wakabayashi I. A subpopulation of fibroblast growth factor-2-binding heparan sulfate is lost in human papillary thyroid carcinomas. *Thyroid* 2000;10: 843–9.
- [37] Brunet LJ, McMahon JA, McMahon AP, Harland RM. Noggin, cartilage morphogenesis, and joint formation in the mammalian skeleton. *Science* 1998;280: 1455–7.

- [38] Bachiller D, Klingensmith J, Kemp C, Belo JA, Anderson RM, May SR, McMahon JA, McMahon AP, Harland RM, Rossant J, De Robertis EM. The organizer factors Chordin and Noggin are required for mouse forebrain development. *Nature* 2000;403: 658–61.
- [39] Iemura S, Yamamoto TS, Takagi C, Uchiyama H, Natsume T, Shimasaki S, Sugino H, Ueno N. Direct binding of follistatin to a complex of bone–morphogenetic protein and its receptor inhibits ventral and epidermal cell fates in early *Xenopus* embryo. *Proc Natl Acad Sci U S A* 1998;95: 9337–42.
- [40] Parisuthiman D, Mochida Y, Duarte WR, Yamauchi M. Biglycan modulates osteoblast differentiation and matrix mineralization. *J Bone Miner Res* 2005;20: 1878–86.
- [41] Viviano BL, Paine–Saunders S, Gasiunas N, Gallagher J, Saunders S. Domain–specific modification of heparan sulfate by Qsulf1 modulates the binding of the bone morphogenetic protein antagonist Noggin. *J Biol Chem* 2004;279: 5604–11.

Figure legends

Fig. 1. Two dimensional electrophoresis analysis of EMD. CBB staining of EMD separated on 2-D PAGE gel (A). The gel was transferred to a PVDF membrane and immunostained with anti-AMEL (B) and anti-BMP2/4 (C) antibodies. The images were matched using Progenesis PG200 software. Merged image (D) shows BMP2/4 (red) and amelogenin (green), with overlapping regions shown in yellow.

Fig. 2. Effects of EMD, amelogenin, and BMP2 on intracellular signaling pathways in osteoblasts. MC3T3-E1 cells were cultured in the presence of either EMD, rAMEL, or BMP2 for 0–60 minutes. Proteins in the cells were immunostained with anti-phospho ERK1/2 (p-ERK1/2) and anti-ERK1/2 antibodies (A), or anti-phospho Smad1/5/8 (p-Smad1/5/8) and anti-Smad5 antibodies (B).

Fig. 3. Binding activities of amelogenin to BMP2. The complexes comprising 0 to 1.0 μ g of rAMEL and 100 ng of BMP2 were affinity-precipitated (AP) by Ni-beads (A). The complexes comprising 100 ng of rAMEL and 0 to 500 ng of BMP2 were immunoprecipitated (IP) by anti-BMP2/4 antibody coupled with protein G plus protein

A agarose (B). After washing with buffer, each recovered bead was electrophoresed, transferred and immunostained with anti-BMP2/4 and Anti-AMEL antibody, respectively.

Fig. 4. Avidity analyses of amelogenin and heparin/heparan sulfate. The avidity of amelogenin and heparin/heparan sulfate was analyzed by examining the binding of rAMEL to heparin beads by performing Western blotting using the anti-rAMEL antibody. The binding affinity of rAMEL for heparin was detected by the incubation of rAMEL with 0–200 μg of heparin acrylic beads (A). The binding intensity between rAMEL and heparin was evaluated by estimating the concentration of the NaCl buffer during the binding (B) (* $p < 0.001$). The binding affinity of rAMEL for heparan sulfate was determined by estimating the amounts of free rAMEL in the rAMEL–heparan sulfate complex mixture (C).

Fig. 5. Influence of amelogenin on the inhibition of the BMP2–induced alkaline phosphatase activities by noggin. MC3T3–E1 cells were cultured in 50 ng/mL BMP2 and/or 0–20 ng/mL rAMEL without noggin (A) or with 400 ng/mL noggin (B). After 14 days, the cells were histochemically stained for ALP activity (* $p < 0.001$).

Fig. 6. Effect of amelogenin on the binding between BMP2 and noggin. The mixture of rAMEL, BMP2, and noggin was immunoprecipitated (IP) with the anti-BMP2/4 antibody coupled with protein G plus protein A agarose, and the recovered precipitate was analyzed by Western blot performed with the anti-noggin antibody.

Supplementary figure 1. 2-D PAGE profile of EMD derived from porcine. EMD separated on 2-D PAGE gel was stained with CBB and the fractions were numbered (A). Based on the results of CBB staining and Western blotting, the pI, molecular weight, and relative volume of each fraction were calculated by Progenesis PG200 Software (B).

Supplementary figure 2. The electric pattern of EMD was changed by the different reducing condition or by the digestion of furin. The EMD samples were reduced in different condition or treated with furin, by which pro-BMP was cleaved. The lane 1 was reduced in the manufacturer's recommended condition by the addition of 50 mM DTT and the incubation at 70°C for 10minutes. The lane 2 was reduced in the strict condition by the addition of 150 mM DTT and the incubation at 95°C for 15 minutes.

The lane 3 was digested by furin at 37°C for 8 hours and reduced in the strict condition. The lane M is the molecular weight marker. These were electrophoresed and immunologically analyzed. The gel on which the lane 1 and 2 were electrophoresed was stained by CBB (A). The EMD samples reduced in the different reducing condition were immunostained with anti-AMEL antibody (B). The EMD samples reduced in the different reducing condition and digested by furin were immunostained with anti-BMP2/4 antibody (C). In the panel A, since the approximate 60 kDa band appeared in the lane 2 instead of disappearance of the 80 and 110 kDa bands in the lane 1, it was suggested that the manufacturer's recommended condition was insufficient in the reducing of EMD. In the panel B, the 80 kDa band immunostained with anti-AMEL antibody in the lane 1 disappeared in the lane2. This observation indicated that the high molecular weight fraction immunostained with anti-AMEL and anti-BMP-2/4 antibody in Figure 1D would be reduced in the strict condition. In the panel C, the approximate 60 kDa band immunostained with anti-BMP-2/4 antibody appeared in the lane2 instead of disappearance of the 80 and 110 kDa bands in the lane 1. Then, the approximate 60 and 18 kDa bands were detected with anti-BMP-2/4 antibody in the lane3. Thus, it was developed that the anti-BMP2/4 antibody positive fraction in EMD shifted from 80 and 110 kDa to approximate 60 kDa by the strict reducing condition and that the 60 kDa of

the anti-BMP2/4 antibody positive band corresponding to the pro-BMP was digested into the approximate 18 kDa band corresponding to the processed BMP.

Fig. 1

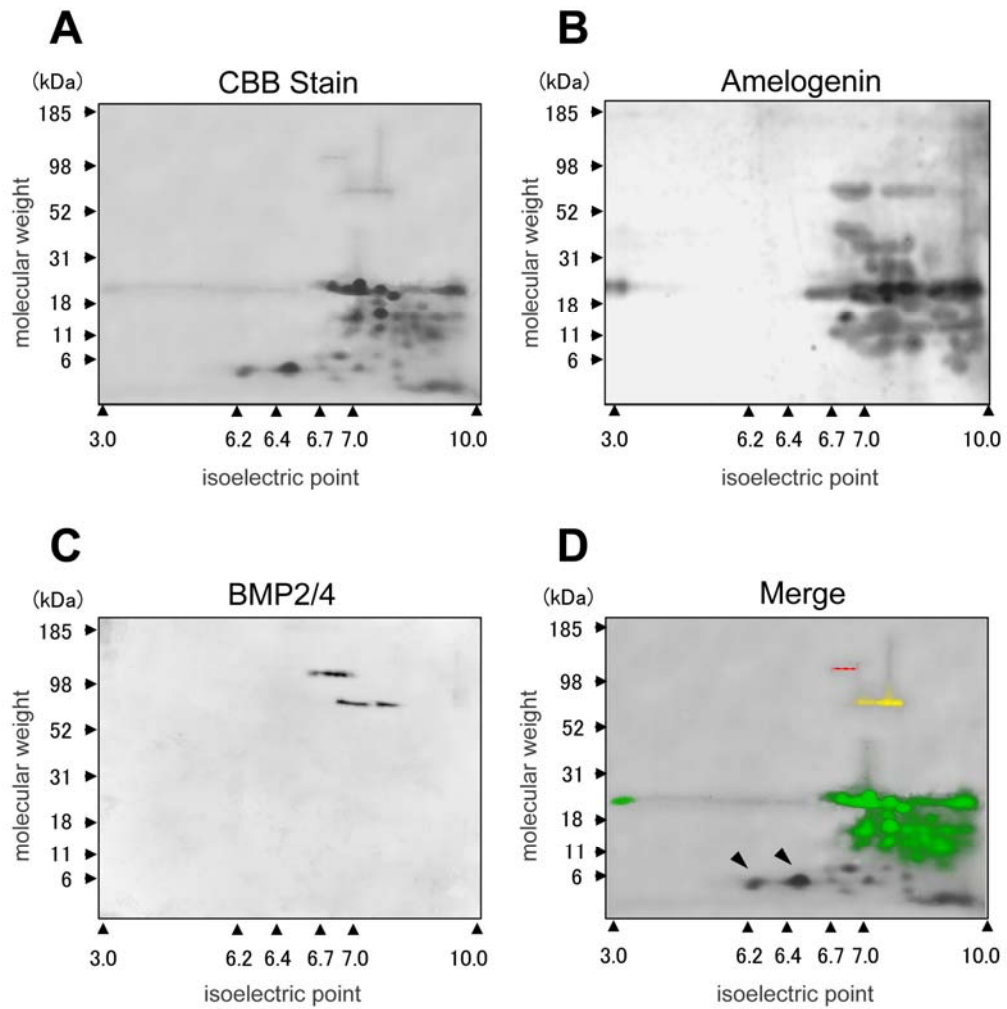


Fig. 2

A

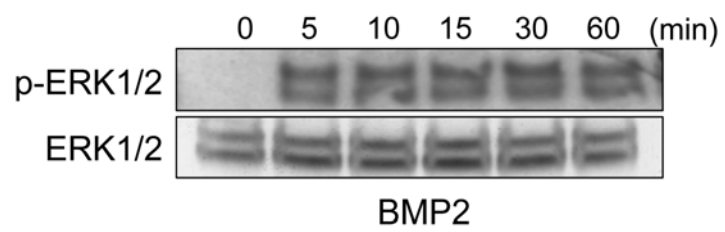
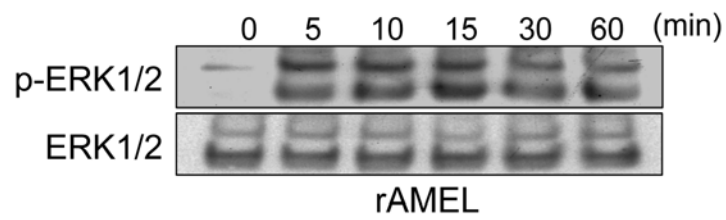
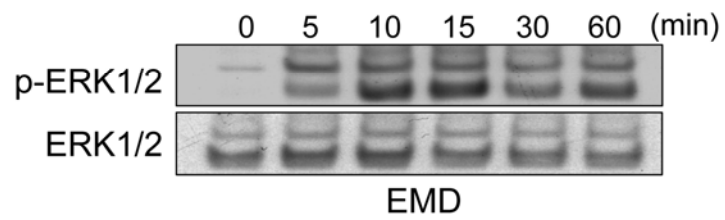


Fig. 2

B

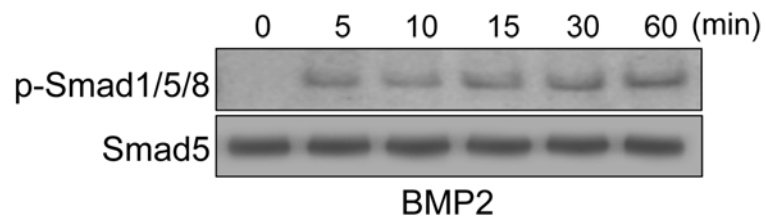
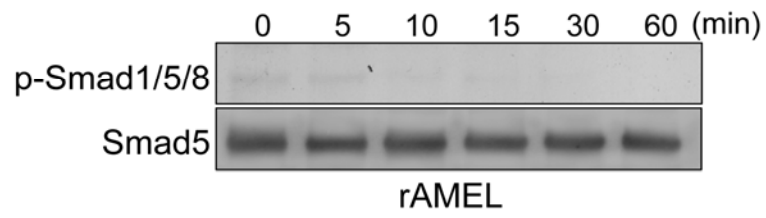
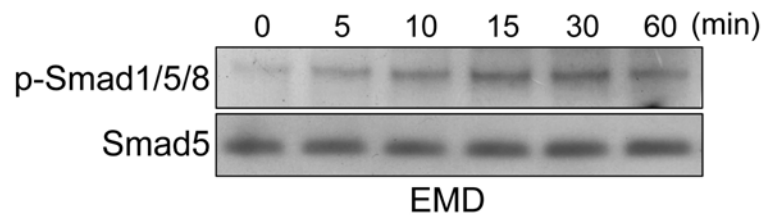
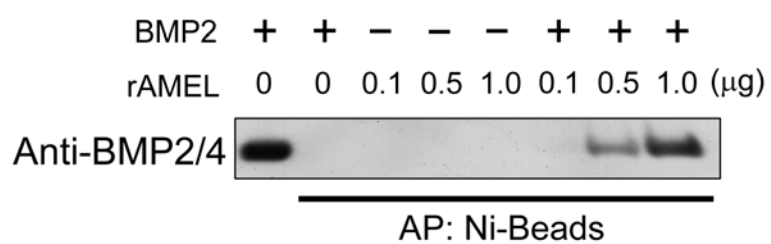


Fig. 3

A



B

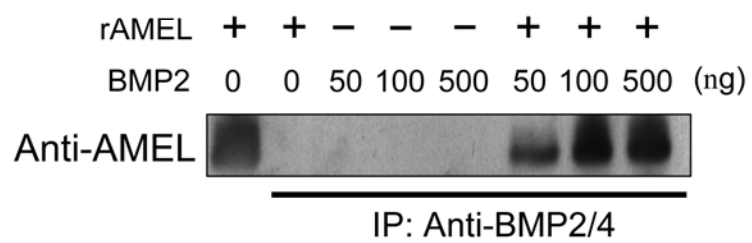
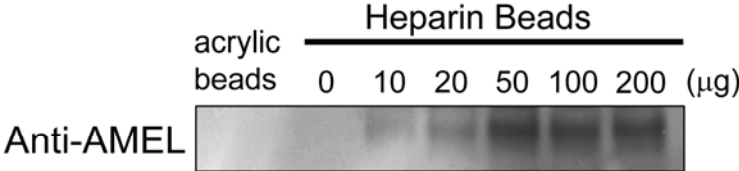
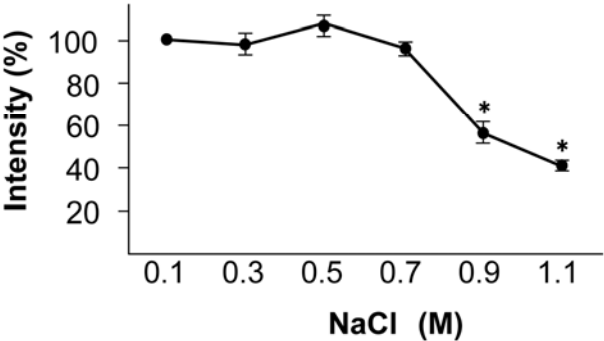
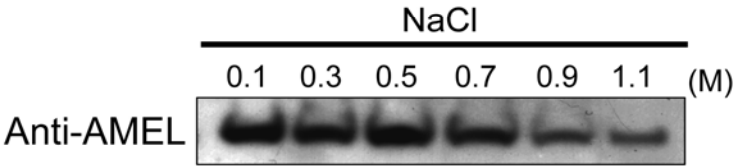


Fig. 4

A



B



C

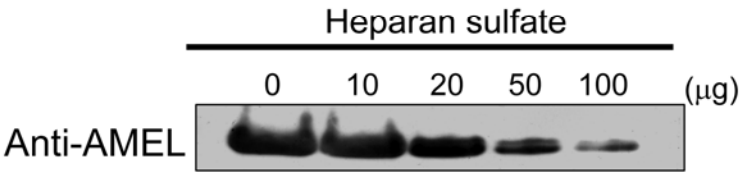
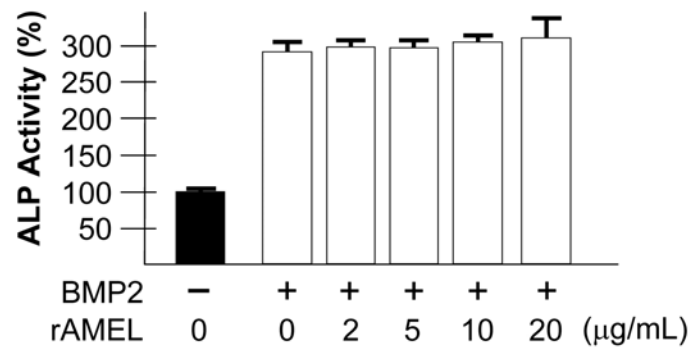


Fig. 5

A



B

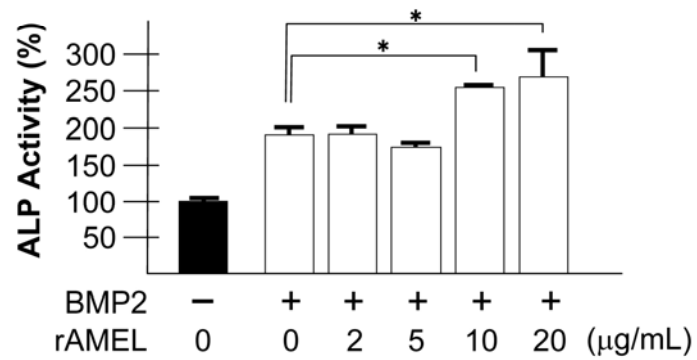
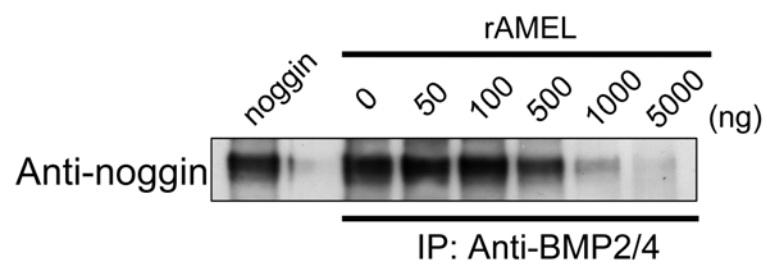
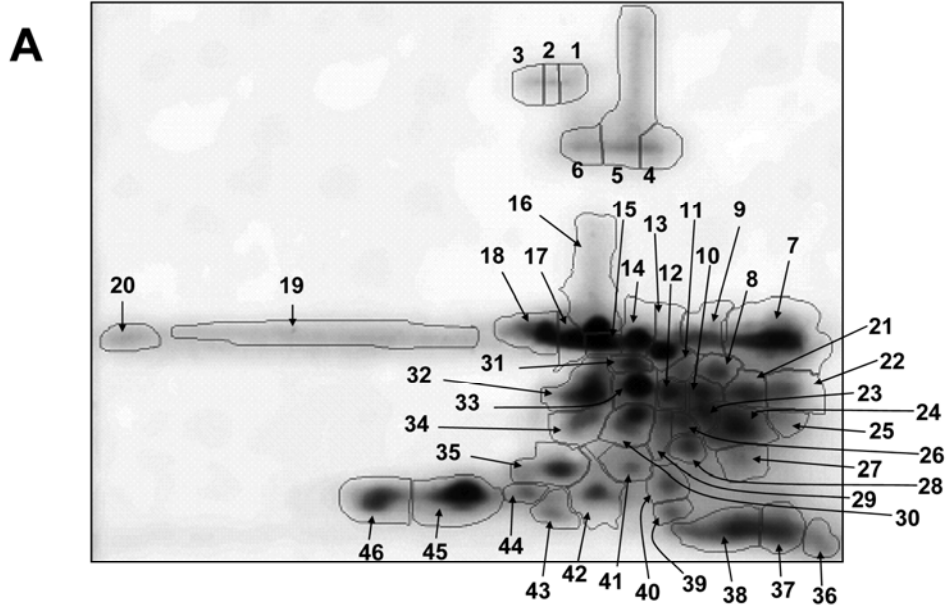


Fig. 6



Supplement-1



B

amelogenin

No.	Vol(%)	pI	MW(kDa)
7	7.4	9.2	23
8	1.5	8.7	18
9	2.2	8.6	24
10	1.6	8.6	15
11	0.8	8.4	18
12	1.6	8.3	15
13	2.5	8.3	22
14	2.3	8.1	24
15	1.5	7.8	22
16	4.3	7.7	32
17	1.7	7.5	23
18	2.7	7.2	24
19	5.1	5.6	24
20	1.1	3.9	23
21	2.1	8.9	15
22	2.4	9.3	15
23	1.0	8.6	12
24	3.7	8.9	11
25	0.9	9.3	12
26	0.9	8.4	12
27	1.8	8.9	8
28	1.3	8.5	9
29	1.3	8.2	11
30	2.6	8.0	12
31	1.1	8.0	19
32	3.8	7.6	16
33	2.7	8.0	16
34	2.1	7.6	12

BMP

No.	Vol(%)	pI	MW(kDa)
1	0.7	7.5	115
2	0.4	7.4	113
3	0.7	7.2	113

BMP + amelogenin

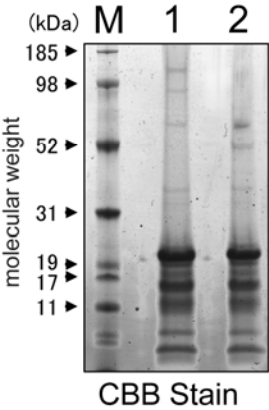
No.	Vol(%)	pI	MW(kDa)
4	1.2	8.2	78
5	4.5	8.0	108
6	1.1	7.6	79

unknown

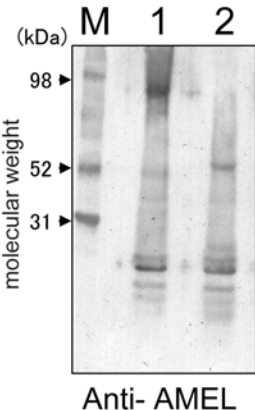
No.	Vol(%)	pI	MW(kDa)
35	2.7	7.4	8
36	1.1	9.5	3
37	2.6	9.2	4
38	4.1	8.8	4
39	0.8	8.3	5
40	1.6	8.3	7
41	1.7	8.0	8
42	2.7	7.7	6
43	1.3	7.4	5
44	0.8	7.1	6
45	5.0	6.6	6
46	3.1	5.9	5

Supplement-2

A



B



C

